

Bulk and surface retarded modes in multilayered structures: Antiparallel magnetization

H. How and C. Vittoria

Department of Electrical and Computer Engineering, Northeastern University, Boston, Massachusetts 02115

(Received 22 August 1988; revised manuscript received 5 December 1988)

The wave dispersion relations of the mixed polariton-photon modes propagating within the bulk and along the surface of a semi-infinite magnetic/nonmagnetic layered structure with an alternating arrangement of the magnetization are calculated. The magnetic layers are magnetized to saturation along the uniaxial anisotropy axis, and the waves are considered to propagate transverse to this axis. The results are contrasted with those calculated for a layered structure in which the magnetization in each layer is parallel to each other. For the antiparallel case there evolve modes of wave propagation which assume different dispersion forms when compared to the parallel case. In the parallel case all dispersion branches that exist in the magnetostatic limit coalesce to a single branch, and we find that in the antiparallel case this coalescence is preceded by formation of degenerate branch pairs before this limit is reached. We find that for the antiparallel case some dispersion bands and curves occur at lower frequencies. This is referred to as the "pushing-down" effect. It is proposed that this "pushing-down" effect is due to the vanishing of the rf demagnetization field within the propagating wave fronts. We also predict a new type of surface propagating mode whose appearance is unique to the Kittel, rather than the Voigt, configuration.

I. INTRODUCTION

In the preceding paper we have calculated the surface mode dispersion relations of the mixed polariton-photon waves within a layered structure where the magnetization in each magnetic layer is aligned parallel to an external field.¹ In this paper we are considering the case in which, in the presence of a uniaxial anisotropy field, the magnetization in each successive magnetic layer is aligned antiparallel to each other.² The intrinsic spectrum of the surface and bulk mode excitations within a layered structure of antiparallel magnetization arrangement is therefore essential in understanding the device performances at optical and microwave frequencies incorporating multilayers in the zero/low-field regime.

Surface and bulk mode dispersions of excitations within a layered structure were first treated by Camley *et al.* in the magnetostatic regime.³ Barnas calculated bulk mode dispersions of a layered structure of infinite extent in the retarded regime⁴ and How and Vittoria considered its surface mode excitations in the same retarded regime for a semi-infinite layered structure.¹ All of the above treatments assumed the magnetization of the magnetic layers to be parallel to each other. This paper extends the above work by considering the case where the magnetization is antiparallel to each other in successive magnetic layers.

Formalism developed in Ref. 1 has been extensively used in this analysis. This involves diagonalizing a transfer matrix \mathbf{T} , incorporating the unimodular property of \mathbf{T} , and then connecting \mathbf{T} with the air/layer and layer/layer boundary conditions.⁵ Since the number of boundary conditions between the interfaces of one period of the layered structure has been doubled when compared to that associated with a parallel magnetization configuration,

the calculation scheme becomes much more involved.

This analysis shows that, for a multilayer with antiparallel arrangement of the magnetization, the pattern of the dispersion bands and curves of the bulk and the surface mode excitations and the packing density of them are roughly the same as in the parallel magnetization case. However significant differences in their dispersion spectra are also recognized as the following. In the antiparallel magnetization case the bulk mode dispersions of the upper bulk-bulk type could have cross-band structure. The bulk mode dispersion bands of the bulk-surface type and the lower bulk-bulk type and the surface mode dispersion curves of the lower surface-bulk type are all tending to form degenerate pairs before they are leading to the magnetostatic regime. The (upper) surface-surface-type curves also tend to form degenerate pairs except for those curves appearing on the positive propagation side for the case of $\epsilon_d = 1$. Here ϵ_d denotes the permittivity of the nonmagnetic layers. The upper and the lower surface-bulk-type modes, while they are reciprocal in the parallel magnetization configuration, could be non-reciprocal with respect to the wave propagation directions. The dispersion curves of the (upper) surface-surface type in the antiparallel magnetization configuration can assume different functional forms, and for $\epsilon_d = 1$ they can even switch the dispersion curves on the two sides of the \mathbf{k} direction as the magnetization changes from parallel to antiparallel configuration. The most intricate change of the excitation spectrum for the case of antiparallel magnetization is the "pushing-down" feature of some of the dispersion band and curves. We notice that the position of the lowest curve in the group of the upper surface-bulk-type modes has been lowered, the lowest band in the group of the upper bulk-bulk-type modes has been pushed down to form a second band of

the bulk-surface-type, and the lowest curve in the group of the lower surface-bulk-type modes has been pushed down to form a single unique surface curve of the "lower" surface-surface type. This new type of surface waves does not appear in the parallel magnetization case and whose dispersion form resembles very much the dispersion curve associated with a single magnetic medium in the Kittel, rather than the Voigt, configuration. This "pushing-down" effect might be explained by the following. In the antiparallel magnetization case the rf positive and negative magnetic charges are alternatively arranged along the sides of the wave fronts such that the rf demagnetization field vanishes. This is a situation analogous to the propagation of the so-called Kittel transverse modes in a single bulk gyromagnetic medium.

II. CALCULATIONS

The geometry of a semi-infinite stack consisting of alternating magnetic and nonmagnetic layers is shown in Fig. 1. Here the easy axis of magnetization directed along the z and the x axis denotes the direction normal to the film. Without applying an external magnetic field we assume, as it is usually the case,² the magnetization in each successive magnetic layer is aligned antiparallel to each other as shown in the figure. The magnetic layers are considered identical, each of which has thickness d_f and optical permeability μ_f . μ_f may differ from unity and assumes contributions from high-frequency magnetic-dipole excitations such as optical magnons. No magnetic exchange interaction will be considered within the magnetic layers. The nonmagnetic layers are as-

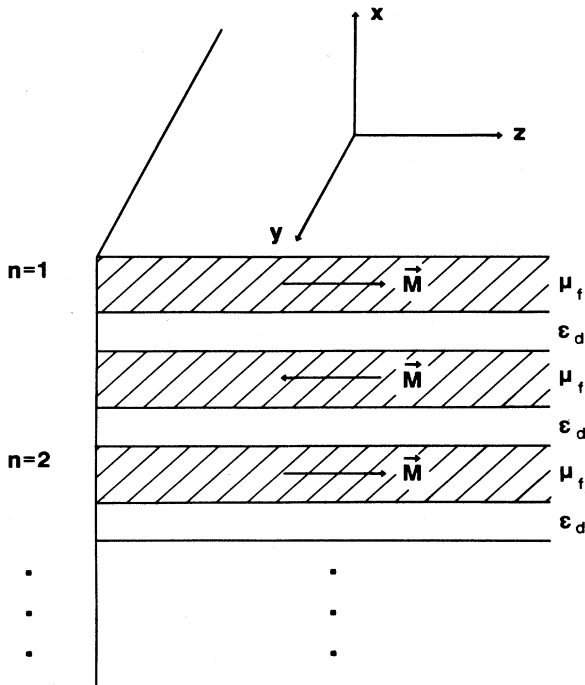


FIG. 1. Geometry configuration of the layered structure with antiparallel magnetization configuration.

sumed to have thickness d_d and permittivity ϵ_d . The period of the layered structure is therefore consisting of two magnetic and two nonmagnetic layers. The waves considered are propagating along the $\pm y$ directions, the Voigt configuration. Gaussian units are used in this analysis.

The effective field associated with a uniaxial anisotropy is

$$\mathbf{H}_0 = \pm \frac{2K}{M_s} \hat{z}, \quad (1)$$

where K is the uniaxial anisotropy constant and M_s denotes saturation magnetization.⁵ Assume \mathbf{H}_0 is parallel to $+\hat{z}$ for the first magnetic layer and is parallel to $-\hat{z}$ for the second one, etc. The formalism developed in Ref. 1 can therefore be directly applied to those odd-numbered magnetic layers. For even-numbered magnetic layers we substitute the following changes:

$$\omega_1 \rightarrow -\omega_1 \quad \text{and} \quad \omega_0 \rightarrow -\omega_0^*.$$

Here

$$\omega_1 = 4\pi\gamma M_0 / \mu_f$$

and

$$\omega_0 = \gamma H_0 - i\alpha\omega$$

with γ and α denoting gyromagnetic ratio and Gilbert damping constant, respectively. The above changes implies that the Polder permeability tensor $\boldsymbol{\mu}$ shall be changed into its complex conjugate $\boldsymbol{\mu}^*$, where

$$\boldsymbol{\mu} = \begin{pmatrix} \mu_1 & i\mu_2 & 0 \\ -i\mu_2 & \mu_1 & 0 \\ 0 & 0 & \mu_f \end{pmatrix} \quad (2)$$

with

$$\mu_1 = \mu_f \left[1 + \frac{\omega_0\omega_1}{\omega_0^2 - \omega^2} \right],$$

and

$$\mu_2 = \mu_f \frac{\omega\omega_1}{\omega_0^2 - \omega^2}.$$

Intuitively the change of the permeability $\boldsymbol{\mu}$ to its complex conjugate $\boldsymbol{\mu}^*$ is associated with the change of rotational sense of the polarizations of the rf fields and is therefore a direct consequence of reversing a static field. Therefore, as long as the rf properties of the layered structure are considered, the system is viewed as composed of alternating magnetic layers of Polder permeability $\boldsymbol{\mu}$ and $\boldsymbol{\mu}^*$ intermediated by nonmagnetic layers.

Define the local vertical coordinate for the n th period of the layered structure by the following:

$$\xi_n = x + 2(n-1)l,$$

where $l = d_d + d_f$ denotes half the period of the layered structure. From Ref. 1 we write the \mathbf{h} field within the n th period of the layered structure as the following:

$$\begin{aligned}
\mathbf{h}_n(\mathbf{r}, t) &= (\mathbf{A}_n e^{-\beta_f \xi_n} + \mathbf{B}_n e^{+\beta_f \xi_n}) e^{i(ky - \omega t)} \quad \text{for } 0 \geq \xi_n \geq -d_f, \\
&= (\mathbf{C}_n e^{-\beta_d \xi_n} + \mathbf{D}_n e^{+\beta_d \xi_n}) e^{i(ky - \omega t)} \quad \text{for } -d_f \geq \xi_n \geq -l, \\
&= (\mathbf{E}_n e^{-\beta_f \xi_n} + \mathbf{F}_n e^{+\beta_f \xi_n}) e^{i(ky - \omega t)} \quad \text{for } -l \geq \xi_n \geq -l - d_f, \\
&= (\mathbf{G}_n e^{-\beta_d \xi_n} + \mathbf{H}_n e^{+\beta_d \xi_n}) e^{i(ky - \omega t)} \quad \text{for } -l - d_f \geq \xi_n \geq -2l.
\end{aligned} \tag{3}$$

Here

$$\beta_f^2 = k^2 - \frac{\omega^2}{c^2} \epsilon_f \mu_v, \tag{4a}$$

$$\beta_d^2 = k^2 - \frac{\omega^2}{c^2} \epsilon_d \mu_d, \tag{4b}$$

with the Voigt permeability μ_v defined by

$$\mu_v = \mu_1 - \mu_2^2 / \mu_1. \tag{5}$$

Note that β_f can be used in Eq. (3) to characterize the field profile within the second magnetic layer of each period only if the Gilbert damping constant α and the conductivity σ_f of the magnetic medium are zero. We shall restrict the following analysis to the case of nondissipative system ($\alpha=0$, $\sigma_f=0$) and take the permittivity of the magnetic medium, ϵ_f , and the permeability of the nonmagnetic medium μ_d both equal to unity.

In Eq. (3) \mathbf{A}_n , \mathbf{B}_n , \mathbf{C}_n , \mathbf{D}_n , \mathbf{E}_n , \mathbf{F}_n , \mathbf{G}_n , and \mathbf{H}_n are constant vectors having components only in the x - y plane. Since the divergence of \mathbf{b} vanishes, this implies that the x and y components of the above vectors are mutually related as the following:

$$\frac{A_{n,x}}{A_{n,y}} = -\frac{F_{n,x}}{F_{n,y}} = -i \frac{\mu_1 k + \mu_2 \beta_f}{\mu_1 \beta_f + \mu_2 k}, \tag{6a}$$

$$\frac{B_{n,x}}{B_{n,y}} = -\frac{E_{n,x}}{E_{n,y}} = i \frac{\mu_1 k - \mu_2 \beta_f}{\mu_1 \beta_f - \mu_2 k}, \tag{6b}$$

$$\frac{C_{n,x}}{C_{n,y}} = \frac{G_{n,x}}{G_{n,y}} = -i \frac{k}{\beta_d}, \tag{6c}$$

$$\frac{D_{n,x}}{D_{n,y}} = \frac{H_{n,x}}{H_{n,y}} = i \frac{k}{\beta_d}. \tag{6d}$$

Here $A_{n,x}$ denotes the x component of vector \mathbf{A}_n , etc. The boundary conditions require $b_{n,x}$ and $h_{n,y}$ to be continuous across the layer boundaries. After matching the boundary conditions at $\xi_n = -d_f$, $\xi_n = -l$, $\xi_n = -l - d_f$, and $\xi_n = -2l$ and having used Eqs. (6a)–(6d), one obtains

$$\begin{pmatrix} A_{n+1,y} \\ B_{n+1,y} \end{pmatrix} = \mathbf{T} \cdot \begin{pmatrix} A_{n,y} \\ B_{n,y} \end{pmatrix}, \tag{7}$$

where the 2×2 transfer matrix \mathbf{T} is defined in the Appendix.

As outlined in Ref. 1 the bulk mode dispersions are derived by utilizing the Bloch theorem and the unimodular property of matrix \mathbf{T} as

$$\cos(2Ql) = \frac{1}{2}(T_{11} + T_{22}). \tag{8}$$

Here Q denotes the one-dimensional wave vector in the reciprocal space conjugate to the one-dimensional vector space of x axis. Surface mode decay constant κ and dispersion relations can be obtained by using Eqs. (17) and (18) in Ref. 1 as

$$\cosh(2\kappa l) = \frac{1}{2}(T_{11} + T_{22}), \tag{9}$$

$$\begin{aligned}
(T_{11} - T_{22}) &\left[\frac{1}{C} + \frac{\beta_a}{A} \right] \left[\frac{-1}{C} + \frac{\beta_a}{B} \right] \\
&+ T_{12} \left[\frac{-1}{C} + \frac{\beta_a}{B} \right]^2 - T_{21} \left[\frac{1}{C} + \frac{\beta_a}{A} \right]^2 = 0.
\end{aligned} \tag{10}$$

Here A , B , and C are defined in the Appendix and β_a is defined by

$$\beta_a^2 = k^2 - \frac{\omega^2}{c^2}, \tag{11}$$

which characterizes photon dispersions in air.

III. SURFACE MODES IN THE MAGNETOSTATIC REGIME

We examine in this section the limit forms of Eq. (10) under magnetostatic approximations. Guided by the previous work¹ dealing with parallel magnetization configuration, we shall be cautious to distinguish any particular permittivity value ϵ_d which may cause the leading term coefficient of the approximation to vanish. This will lead us to a subsidiary asymptotic form of the dispersion relations. Magnetostatic approximations take the following form:

$$\beta_a \sim \beta_d \sim \beta_f \sim k \quad (\gg \omega/c). \tag{12}$$

Before directly substituting Eq. (12) into Eq. (10), we examine the coefficient of the leading term, $\exp(2\beta_d d_d + 2\beta_f d_f)$. For large values of β_d and β_f , the leading term assumes much larger value than the rest of the terms and the zeros of Eq. (10) is determined roughly by the vanishing condition of its coefficient. The leading term coefficient can be written in the following factorized form, which is then set to zero, as

$$\begin{aligned}
(\beta_d - \beta_a)(\omega_0 - \omega) &\left[\omega_0 \pm \omega + \frac{1}{1 + 1/\mu_f} \right]^2 \\
&\times \left[\omega_0 \mp \omega + \frac{1}{1 + 1/\mu_f} \right]^2 = 0,
\end{aligned} \tag{13}$$

where the upper (lower) sign before ω denotes surface wave propagation in the positive (negative) direction of y

axis. Therefore Eq. (13) can truly determine asymptotically the surface wave dispersions in the large k limit only if β_d is not equal to β_a , i.e., ϵ_d is not equal to unity. Note that in deriving Eq. (13) we have assumed the frequency ω to be different from ω_v and ω_v is defined by

$$\omega_v = [\omega_0(\omega_0 + \omega_1)]^{1/2}.$$

ω_v is the resonance frequency in Voigt configuration into which there are infinitely many bulk and surface modes condensed in the magnetostatic limit.

When β_d equals β_a , the asymptotic dispersion form of Eq. (10) is determined by the next nonvanishing term in Eq. (10). When the magnetostatic limit, Eq. (12), has been substituted into Eq. (10), one finds the nonvanishing leading term is $\exp(2kd_f)$ and its coefficient, when set to zero, is

$$(\omega_0 - \omega) \left[\omega_0 \mp \omega + \frac{\omega_1}{1 + 1/\mu_f} \right] \left[\omega_0 \mp \omega + \frac{\omega_1}{1 - 1/\mu_f} \right] \times \left[\omega_0 \pm \omega + \frac{\omega_1}{1 + 1/\mu_f} \right]^2 = 0. \quad (14)$$

Here, again, the upper (lower) sign before ω denotes surface wave propagation in the positive (negative) direction of y axis.

Therefore, depending on the permittivity value of the nonmagnetic layers, there are two kinds of asymptotic forms that the surface mode dispersion curves can approach in the magnetostatic limit. For surface waves propagating in the negative direction, both Eqs. (13) and (14) dictate the same asymptotic frequencies

$$\omega = \omega_0, \quad (15a)$$

$$\omega = \omega_0 + \frac{\omega_1}{1 + 1/\mu_f} \text{ doubly degenerate.} \quad (15b)$$

For surface waves propagating in the positive direction, Eq. (13) and (14) give different asymptotic frequencies

$$\omega = \omega_0, \quad (16a)$$

$$\omega = \omega_0 + \frac{\omega_1}{1 + 1/\mu_f} \text{ doubly degenerate,} \quad (16b)$$

for $\epsilon_d > 1$, and

$$\omega = \omega_0, \quad (17a)$$

$$\omega = \omega_0 + \frac{\omega_1}{1 + 1/\mu_f}, \quad (17b)$$

$$\omega = \omega_0 + \frac{\omega_1}{1 - 1/\mu_f}, \quad (17c)$$

for $\epsilon_d = 1$. A comparison of Eqs. (15b), (16b), (17b), and (17c) reveals that the propagation of surface modes (of the surface-surface type) shows more degree of nonreciprocity with respect to wave propagation directions for the case $\epsilon_d = 1$ than for the other cases $\epsilon_d > 1$.

Dimensionless parameters, denoted by "tilded" letters, are introduced for plotting the dispersion relations, Eqs.

(9) and (10). We normalize frequencies by ω_1 and wave vectors by ω_1/c . It follows that

$$\tilde{\omega}_0 = \omega_0/\omega_1,$$

$$\tilde{\omega} = \omega/\omega_1,$$

$$\tilde{k} = k/(\omega_1/c),$$

$$\tilde{d}_f = d_f(\omega_1/c),$$

$$\tilde{d}_d = d_d(\omega_1/c).$$

In order to have a closer comparison with the results in Ref. 1, we choose $\tilde{\omega}$ to be 2 for all the dispersion plots.

IV. CALCULATIONAL RESULTS

A general description about the bulk and the surface mode dispersion bands and curves in a layered structure is introduced first. With the translational symmetry of multilayers the bulk mode dispersions form banded structures.^{1,4} This is similar to the formation of energy bands that atomic energy levels interact within a three-dimensional lattice array of atoms. Bulk mode bands can be distinguished in three types. The upper bulk-bulk type consists of infinitely many bulk bands which are confined in the retarded regime and above the line defining magnetostatic limit, $\omega = \omega_v$. The lower bulk-bulk type also consists of infinitely many bulk bands; they exist in below the line defining magnetostatic limit and in the magnetostatic limit they all collapse into a single frequency ω_v . The bulk-surface type consists of only finite number of bulk bands whose width is very narrow compared to those of other bulk mode types. The bulk-surface-type modes are all convergent to Damon-Eshbach waves in the magnetostatic regime. Four types of dispersion curves are found for the surface modes propagating along the surface of a layered structure. The upper surface-bulk-type modes and the lower surface-bulk-type modes exist, respectively, in between every two upper and lower bulk-bulk-type dispersion bands. However, the upper surface-bulk-type modes may not show up in a layered structure depending on the relative magnitudes of ϵ_d and μ_f . The (upper) surface-surface type of surface modes consists only of finite number of dispersion curves which, in the magnetostatic limit, may converge to different limit frequencies as assumed by a Damon-Eshbach wave. The propagation of the (upper) surface-surface-type modes can show, in general, a great deal of nonreciprocity with respect to the wave propagation directions. The above descriptions are valid for a general layered structure regardless of its magnetization configurations (parallel or antiparallel). There remains another type for surface mode dispersions, the "lower" surface-surface type, which is unique to a layered structure with antiparallel magnetization.

Figures 2–5 show dispersion bands and curves of the bulk and the surface modes in a layered structure with antiparallel magnetization configuration. In these plots μ_f and ϵ_d assume, respectively, the values of 1.5 and 2.0 for Figs. 2–4 and 1.75 and 1.0 for Fig. 5. These are the cases which were originally chosen in Ref. 1. In the

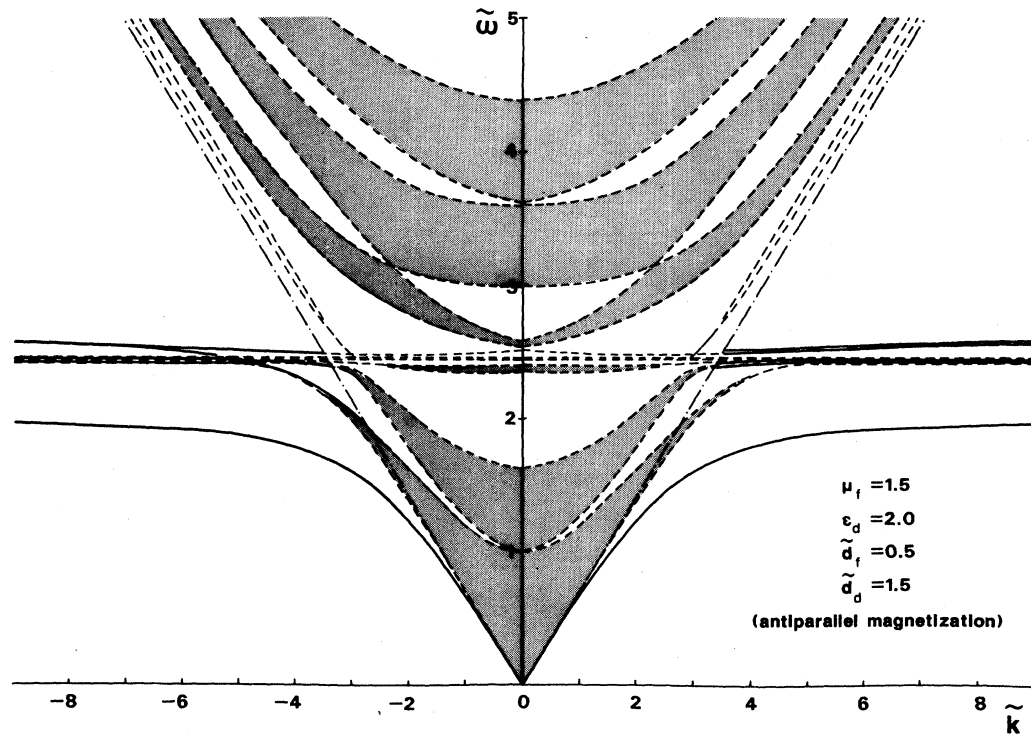


FIG. 2. Dispersions for a layered structure in the antiparallel magnetization configuration: $\mu_f = 1.5$, $\epsilon_d = 2.0$, $\tilde{d}_f = 0.5$, $\tilde{d}_d = 1.5$.

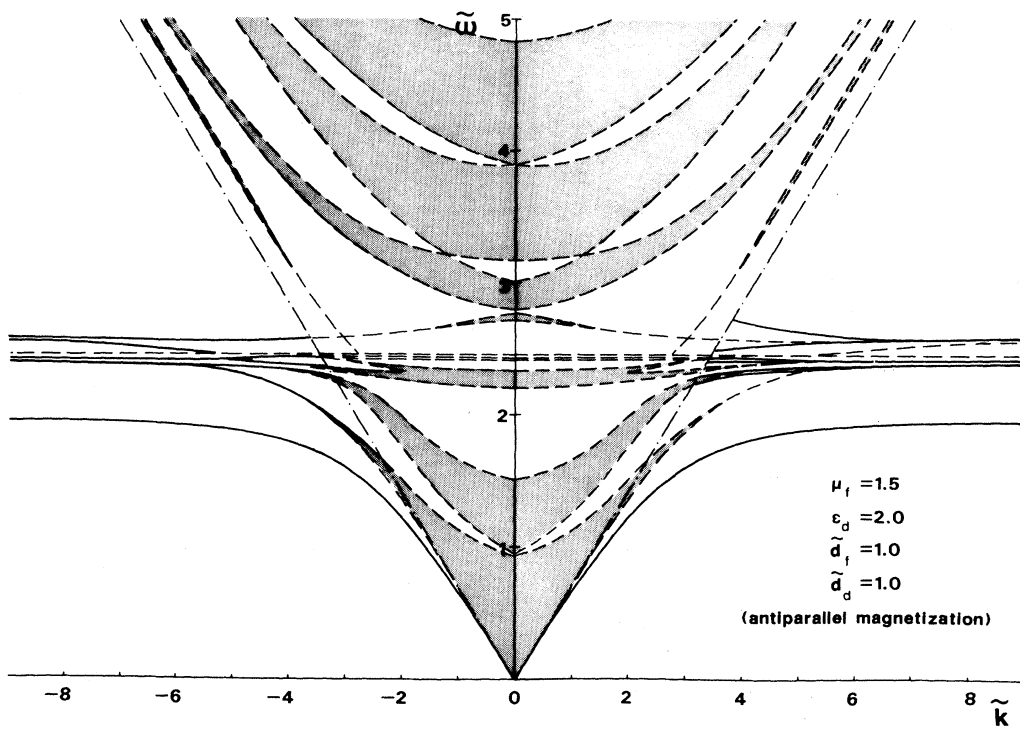


FIG. 3. Dispersions for a layered structure in the antiparallel magnetization configuration: $\mu_f = 1.5$, $\epsilon_d = 2.0$, $\tilde{d}_f = 1.0$, $\tilde{d}_d = 1.0$.

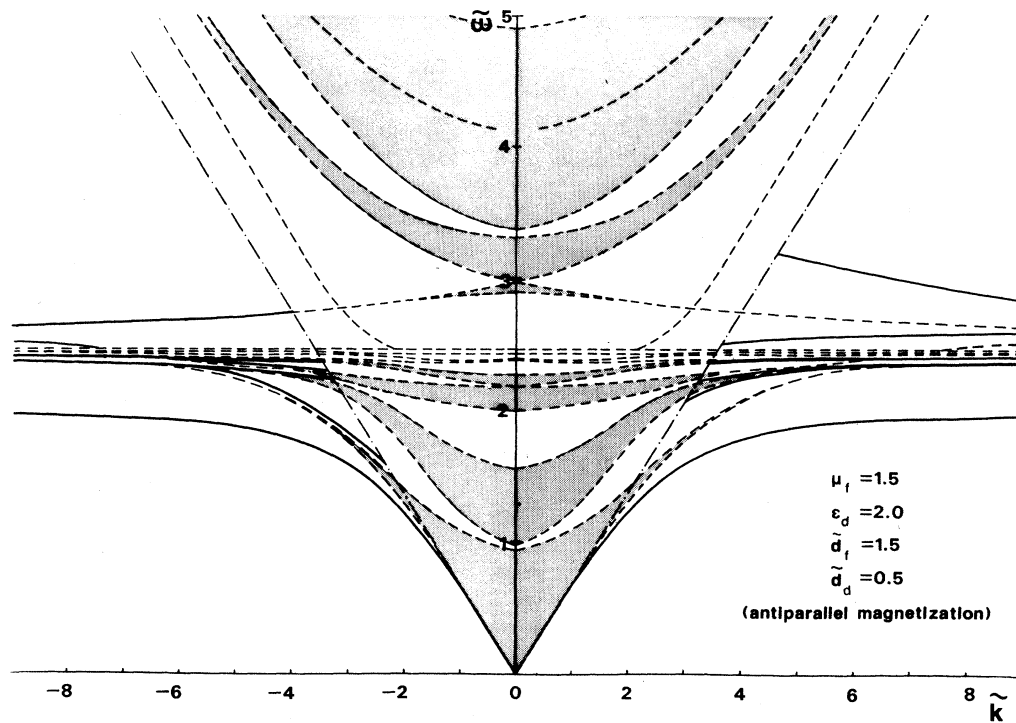


FIG. 4. Dispersions for a layered structure in the antiparallel magnetization configuration: $\mu_f = 1.5$, $\epsilon_d = 2.0$, $\tilde{d}_f = 1.5$, $\tilde{d}_d = 0.5$.

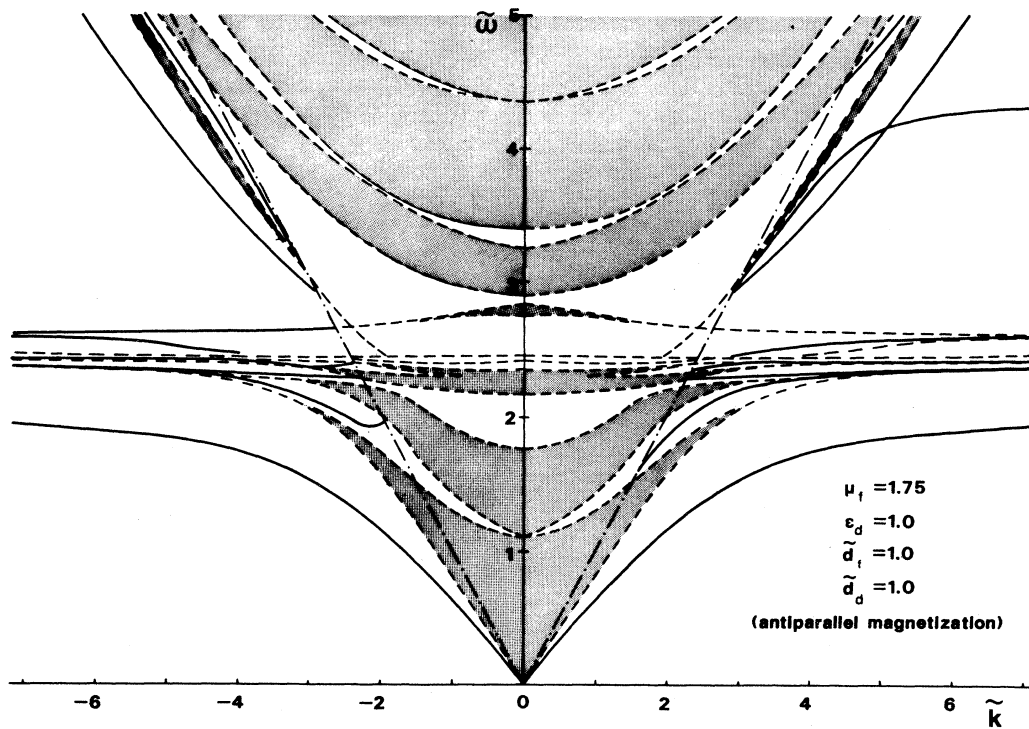


FIG. 5. Dispersions for a layered structure in the antiparallel magnetization configuration: $\mu_f = 1.75$, $\epsilon_d = 1.0$, $\tilde{d}_f = 1.0$, $\tilde{d}_d = 1.0$.

figures, bulk mode dispersions are shown as shaded bands bounded by dashed lines, surface mode dispersions are shown in solid lines, and the dashed-dotted lines represent the light cones for the nonmagnetic medium. A comparison of these plots with those corresponding ones in Ref. 1 shows that the packing densities of the dispersion bands and curves are roughly the same for both magnetization configurations. As the ratio of \bar{d}_f to \bar{d}_d increases from Figs. 2–4, the packing density of the bands and the curves increases in as much as the same way that packing density, increases in Ref. 1. Note that the upper surface-bulk-type modes appear only in Fig. 5. The condition that a upper surface-surface-type mode can appear in a layered structure, regardless of its magnetization configurations, is that the (optical) permeability of the magnetic medium μ_f is larger than the permittivity of the nonmagnetic medium ϵ_d . This is a situation analogous to the occurrence of those negatively propagating surface waves in a single gyromagnetic medium as discussed by Hartstein.⁶

Three remarkable changes associated with bulk mode dispersion bands are noticed in these figures when compared to the figures shown in Ref. 1. First, the bulk mode dispersions can have cross-band structure for the upper bulk-bulk-type modes as indicated in Figs. 2 and 3. Second, the bands of the bulk-surface type and the lower bulk-bulk type tend to form a two-fold degeneracy for the high k limit—the magnetostatic limit. This double-degeneracy tendency of dispersion bands (also curves) seems to arise from the fact that the unit cell for the antiparallel magnetization case has been doubled when compared to that associated with the parallel magnetization case. Third, the lowest band in the group of the upper bulk-bulk-type bands has been pushed down to form a band of the bulk-surface type. It then joins the other bulk-surface-type band as a degenerate pair in the magnetostatic limit. This “pushing-down” feature of bulk bands is shared with some other surface dispersion curves in the antiparallel magnetization configuration and will be discussed later.

Four major differences are found for surface mode dispersion curves in Figs. 2 to 5 for the antiparallel magnetization configuration of a layered structure. First, similar to the bulk-surface-type and the lower bulk-bulk-type bands, the surface dispersion curves of the (upper) surface-surface-type (for negative propagation wave only) and the lower surface-bulk type tend to form degenerate pairs before they go to the magnetostatic limit. The (upper) surface-surface-type curves propagating in the positive directions tend to form pairs only if $\epsilon_d > 1$. Second, not all of the upper and the lower surface-bulk dispersion curves show reciprocity with respect to wave propagation directions. It appears that reciprocal and nonreciprocal curves are arranged alternately in these figures. Third, the (upper) surface-surface-type curves may assume different functional forms as compared with the parallel magnetization case. For $\epsilon_d = 2.0$, all the (upper) surface-surface-type modes in the antiparallel magnetization configuration converge to, in the magnetostatic limit, Damon-Eshbach waves with the limit frequency $\bar{\omega} = 2.6$ for both positive and negative propaga-

tion waves, see Figs. 2–4. For the parallel magnetization case with the same ϵ_d value the surface-surface-type modes have different asymptotic frequencies for the two $\pm k$ propagation directions: $\bar{\omega} = 2.6$ for $+k$ direction and $\bar{\omega} = 3.0$ for $-k$ direction, see Figs. 3–5 in Ref. 1. For $\epsilon_d = 1.0$ and in the antiparallel magnetization case, Fig. 5, three (upper) surface-surface-type curves, one for $+k$ direction and two for $-k$ direction, converge in the magnetostatic limit to Damon-Eshbach waves with the limit frequency $\bar{\omega} = 2.636$. The other (upper) surface-surface-type curve in the $+k$ direction converge to $\bar{\omega} = 4.333$ in the magnetostatic limit. This is contrasted with the parallel magnetization case that the curve converging to a Damon-Eshbach wave is shown on the $+k$ side of the dispersion plot, while the curve with limit frequency $\bar{\omega} = 4.333$ appears, instead, on the other side of $-k$ direction, see Fig. 6 of Ref. 1.

The fourth difference is the “pushing-down” effect of some of the dispersion curves. We notice in Fig. 5 that the position of the lowest curve in the group of the upper surface-bulk-type curves has been lowered when compared with that corresponding curve in Fig. 6 of Ref. 1. Furthermore, as shown in Figs. 2–5, the lowest curve in the group of the lower surface-bulk-type curves has been pushed down outside the surface-bulk-type dispersion region. It becomes a curve of the surface-surface-type. We call it the “lower” surface-surface-type curve as to distinguish it from the other (upper) surface-surface-type curves. The lower surface-surface-type curve is unique to a layered structure which appears only in the antiparallel magnetization configuration. Unlike other surface-surface-type curves the lower surface-surface-type curve is reciprocal with respect to wave propagation directions, and it does not couple to any other curves in the magnetostatic limit. The lower surface-surface-type curve converges in the magnetostatic limit to the frequency ω_0 , which is recognized as the Kittel resonance frequency characterizing uniquely the propagation waves in the Kittel configuration. In the Kittel (Voigt) configuration, waves are propagating longitudinal (transverse) to the applied field. Therefore it is quite surprising that the Kittel frequency can even appear in the Voigt configuration

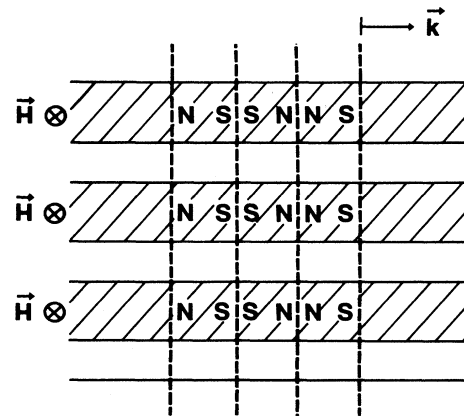


FIG. 6. Demagnetization configuration of the layered structure: parallel magnetization.

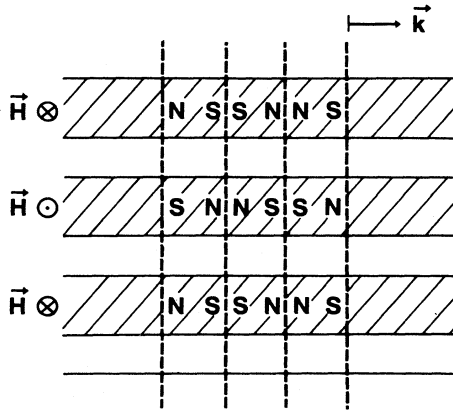


FIG. 7. Demagnetization configuration of the layered structure: antiparallel magnetization.

behaving as a limit frequency such as resonance. Note also that these lower surface-surface-type curves shown in Figs. 2-5 can be quite well approximated by the following relation:

$$k^2 = \frac{\omega^2}{c^2} (\mu_1 + \mu_2),$$

which is the polariton dispersion relation of a single bulk gyromagnetic medium in the Kittel configuration.⁷

Denote θ as the angle between the wave propagation direction and the applied field. The resonance frequency for a wave propagation angle θ is⁷

$$\omega_R = [\omega_0(\omega_0 + \omega_1 \sin^2 \theta)]^{1/2}.$$

The reason that ω_R is increasing with θ is that the effective rf demagnetizing field induced by the wave fronts is increasing with the decreasing angle θ . Maximum rf demagnetization field occurs for $\theta = 90^\circ$ (Voigt configuration) and it vanishes when $\theta = 0^\circ$ (Kittel configuration). For a layered structure with parallel magnetization arrangement and with waves propagating in the Voigt configuration the wave fronts cause periodic changes in the rf magnetic charges within a layer so that

maximum rf demagnetization field is induced. This is indicated in Fig. 6, where wave fronts are shown as dashed lines and the magnetic layers as shaded regions. For the antiparallel magnetization case the rf magnetic charges are again periodically arranged within a given layer, but the induced demagnetization fields in successive layers are oppositely aligned, see Fig. 7. This induces effectively zero rf demagnetization fields and explains why the Kittel frequency is recovered in the Voigt configuration for the antiparallel magnetization case. Other "pushing-down" effects associated with the lowest upper bulk-bulk-type band and the lowest upper surface-bulk-type curve might also be explained by this effect.

V. CONCLUSIONS

A layered structure with antiparallel arrangement of magnetization shows a number of differences in its wave dispersion spectrum when compared to that with parallel magnetization arrangement. These include the cross-band behavior of the upper bulk-bulk-type bands, the pairing nature of the lower bulk-bulk-type and the bulk-surface-type bands, and the lower surface-bulk-type and some of the upper surface-surface-type curves, nonreciprocity of some of the upper and the lower surface-bulk-type curves, different dispersion forms of the upper surface-surface-type curves (even interchange the dispersion curves for the $\pm k$ propagation directions for $\epsilon_d = 1$), and the "pushing-down" feature of the lowest upper bulk-bulk-type band, the lowest upper surface-bulk-type curve, and the lowest lower surface-bulk-type curve. The last feature even causes the appearance of a new dispersion curve of the lower surface-surface type. The "pushing-down" feature is explained by the vanishing of the rf volume demagnetizing field within the wave fronts by means of the alternating rf north and south magnetic charges.

ACKNOWLEDGMENTS

The authors would like to acknowledge the Office of Naval Research (Contract No. N00014-87-K-0041) in sponsoring this research program.

APPENDIX

$$T_{11} = W \{ e^{2\beta_f d_f} [(1+v)^2 e^{\beta_d d_d} - (1-v)^2 e^{-\beta_d d_d}] [(1+u)^2 e^{\beta_d d_d} - (1-u)^2 e^{-\beta_d d_d}] \\ - [(1-u)(1+v) e^{\beta_d d_d} - (1+u)(1-v) e^{-\beta_d d_d}] [(1+u)(1-v) e^{\beta_d d_d} - (1-u)(1+v) e^{-\beta_d d_d}] \},$$

$$T_{12} = W \{ e^{-2\beta_f d_f} [-(1-u)^2 e^{\beta_d d_d} + (1+u)^2 e^{-\beta_d d_d}] [(1+u)(1-v) e^{\beta_d d_d} - (1-u)(1+v) e^{-\beta_d d_d}] \\ + [(1-u)(1+v) e^{\beta_d d_d} - (1+u)(1-v) e^{-\beta_d d_d}] [(1+u)^2 e^{\beta_d d_d} - (1-u)^2 e^{-\beta_d d_d}] \},$$

$$T_{21} = W \{ e^{2\beta_f d_f} [(1+v)^2 e^{\beta_d d_d} - (1-v)^2 e^{-\beta_d d_d}] [-(1+u)(1-v) e^{\beta_d d_d} + (1-u)(1+v) e^{-\beta_d d_d}] \\ + [-(1-u)(1+v) e^{\beta_d d_d} + (1+u)(1-v) e^{-\beta_d d_d}] [-(1-v)^2 e^{\beta_d d_d} + (1+v)^2 e^{-\beta_d d_d}] \},$$

$$T_{22} = W \{ e^{-2\beta_f d_f} [(1-u)^2 e^{\beta_d d_d} - (1+u)^2 e^{-\beta_d d_d}] [(1-v)^2 e^{\beta_d d_d} - (1+v)^2 e^{-\beta_d d_d}] \\ - [(1-u)(1+v) e^{\beta_d d_d} - (1+u)(1-v) e^{-\beta_d d_d}] [(1+u)(1-v) e^{\beta_d d_d} - (1-u)(1+v) e^{-\beta_d d_d}] \} .$$

$$W = \left[\frac{AB}{4\beta_f \beta_d \mu_1 C} \right]^2, \quad u = \beta_d \frac{C}{B}, \quad v = \beta_d \frac{C}{A}$$

and A , B , and C are

$$A = \mu_1 \beta_f - \mu_2 k, \quad B = \mu_1 \beta_f + \mu_2 k, \quad C = \mu_1^2 - \mu_2^2 .$$

¹H. How and C. Vittoria, preceding paper, Phys. Rev. B **39**, 6823 (1989).

²J. J. Krebs, C. Vittoria, G. T. Jonker, and G. A. Prinz, Magn. Mater. **54-57**, 811 (1986); K. Sun and C. Vittoria (unpublished).

³R. E. Camley, T. S. Rahman, and D. L. Mills, Phys. Rev. B **27**, 261 (1983).

⁴J. Barnas, Solid State Commun. **61**, 405 (1987).

⁵C. Vittoria, Phys. Rev. B **32**, 1679 (1985).

⁶A. Hartstein, E. Burstein, A. A. Maradudin, R. Brewer, and R. F. Wallis, J. Phys. C **6**, 1266 (1973).

⁷B. Lax and K. J. Botton, *Microwave Ferrites and Ferrimagnetics* (McGraw-Hill, New York, 1964).

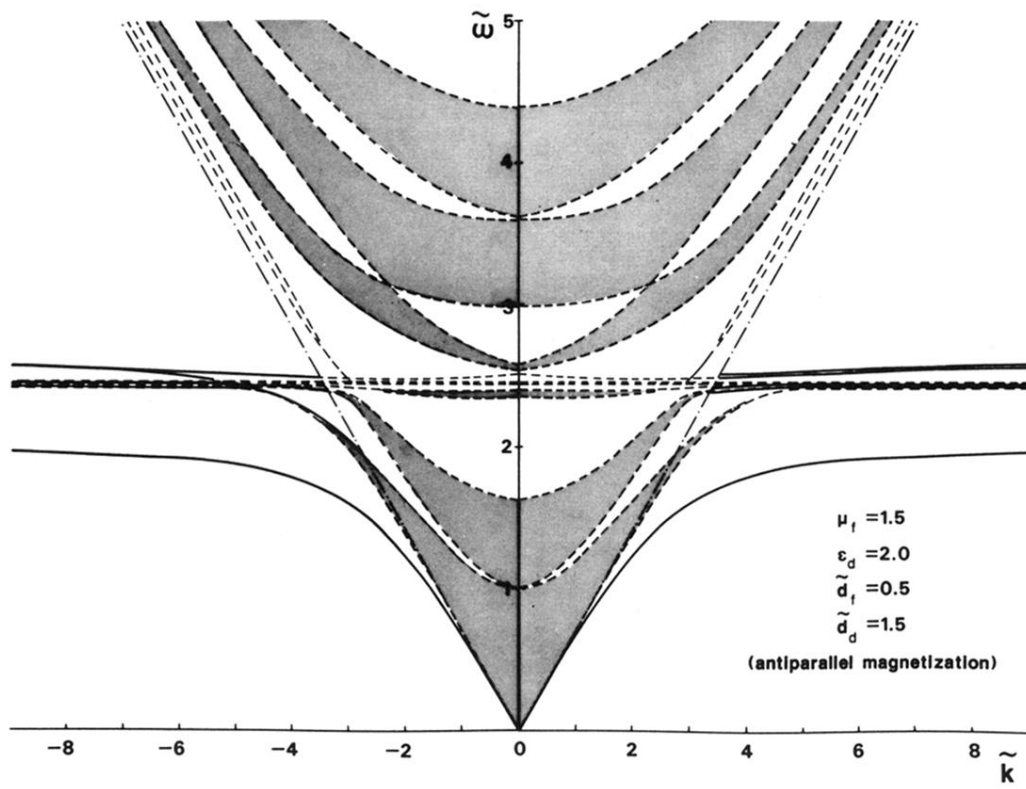


FIG. 2. Dispersions for a layered structure in the antiparallel magnetization configuration: $\mu_f=1.5$, $\epsilon_d=2.0$, $\tilde{d}_f=0.5$, $\tilde{d}_d=1.5$.

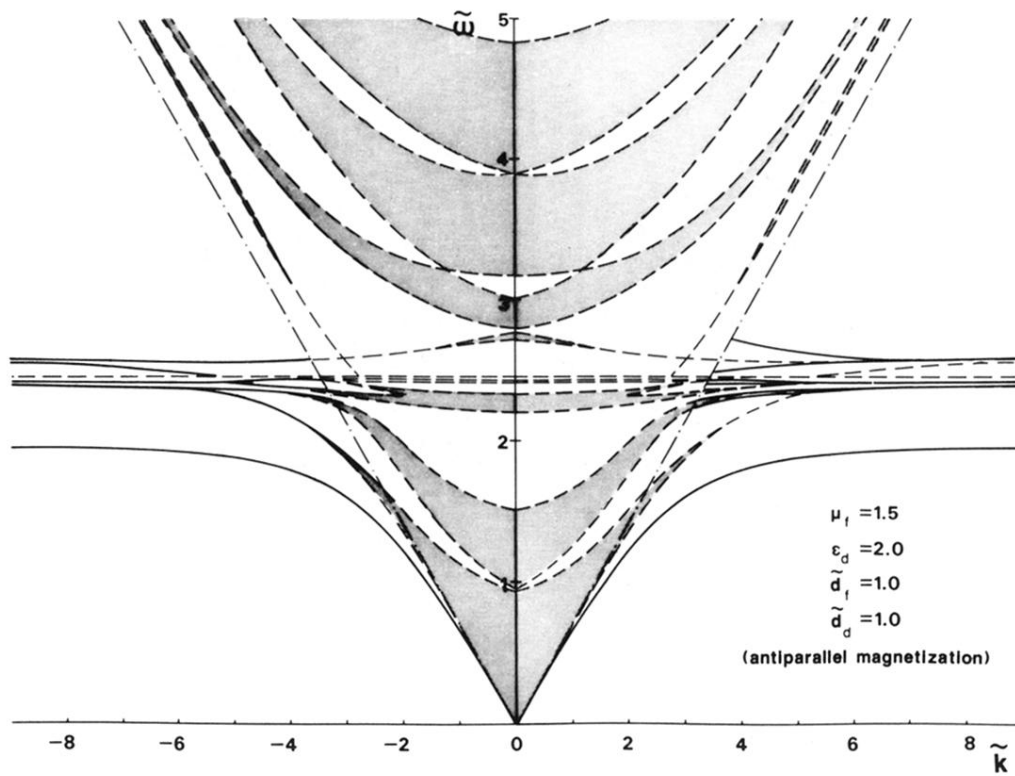


FIG. 3. Dispersions for a layered structure in the antiparallel magnetization configuration: $\mu_f=1.5$, $\epsilon_d=2.0$, $\tilde{d}_f=1.0$, $\tilde{d}_d=1.0$.

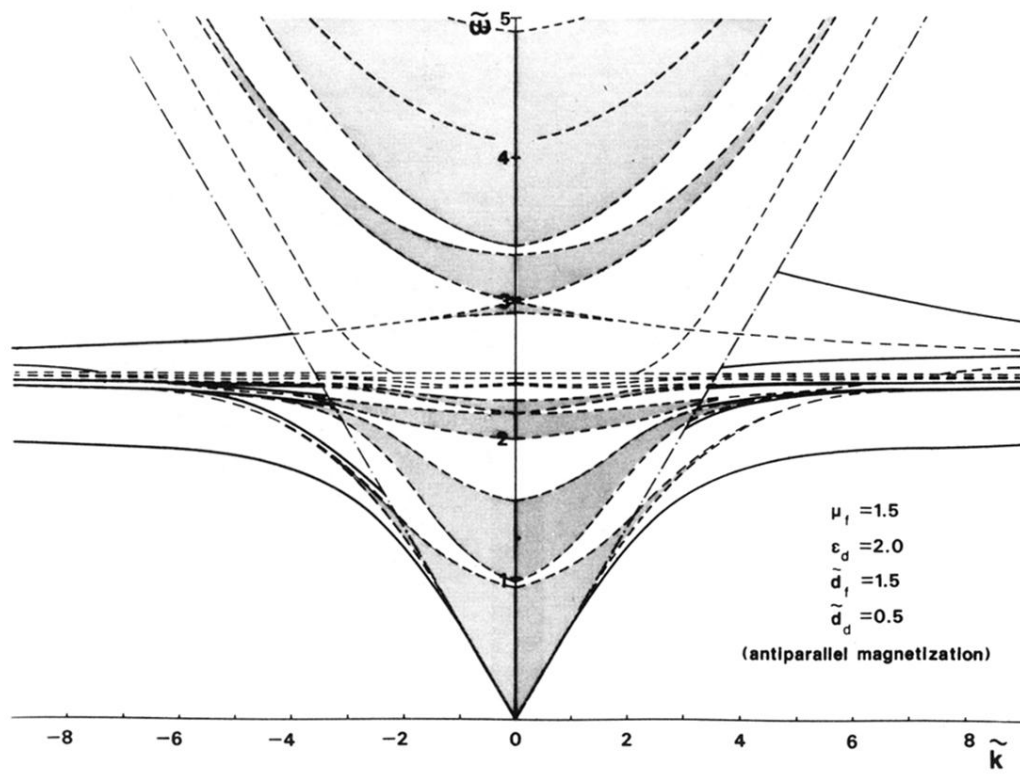


FIG. 4. Dispersions for a layered structure in the antiparallel magnetization configuration: $\mu_f = 1.5$, $\epsilon_d = 2.0$, $\tilde{d}_f = 1.5$, $\tilde{d}_d = 0.5$.

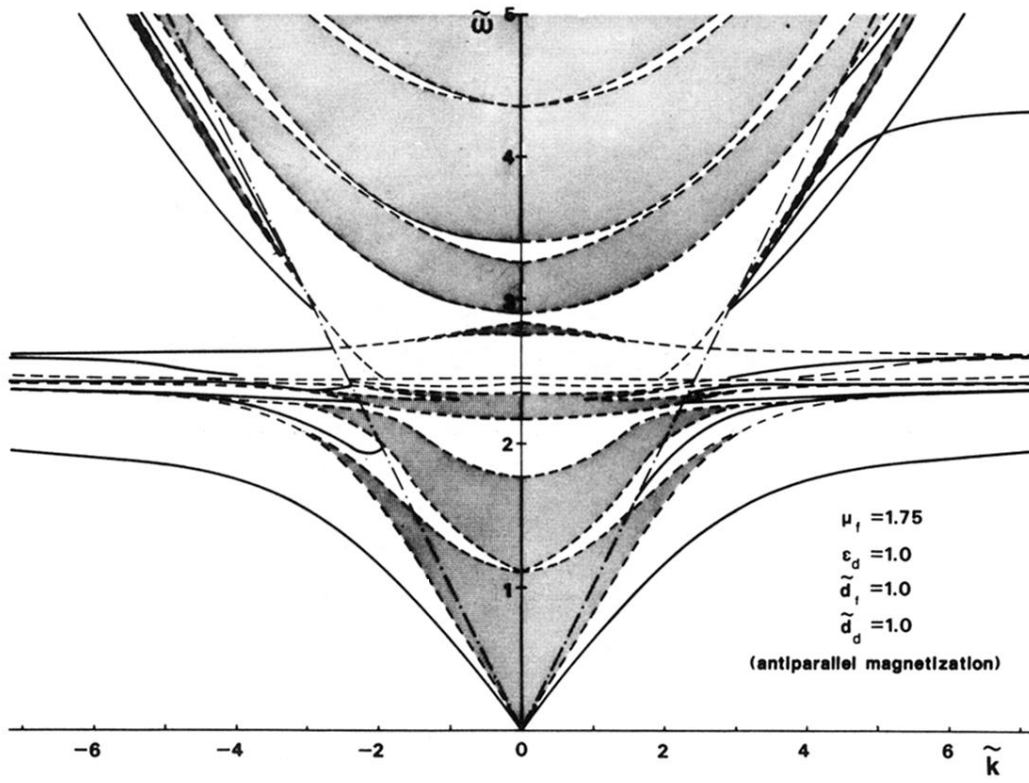


FIG. 5. Dispersions for a layered structure in the antiparallel magnetization configuration: $\mu_f = 1.75$, $\epsilon_d = 1.0$, $\tilde{d}_f = 1.0$, $\tilde{d}_d = 1.0$.